Microstructure/Phase Evolution in Mechanical Alloying/Milling of Stainless Steel and Aluminum Powder Blends

P.P. CHATTOPADHYAY, A. SAMANTA, W. LOJKOWSKI, H.-J. FECHT, and I. MANNA

The present study aims to examine the phase evolution in blends comprising different proportions of stainless steel (316SS) and Al (0, 25, 65, and 85 wt pct) powders during high-energy ball milling through X-ray diffraction (XRD) analysis, scanning electron microscopy (SEM), differential scanning calorimetry (DSC), and high-resolution transmission electron microscopy (HRTEM). An attempt has also been made to study the hardness value of the bulk samples obtained by hot pressing the ball-milled powder blend at suitable temperature and pressure. The results on changes in the constituent phases and hardness value of the bulk samples obtained after consolidation of ball-milled alloy using the high-pressure technique have been reported.

DOI: 10.1007/s11661-007-9206-6

I. INTRODUCTION

MECHANICAL alloying (MA) is a convenient and inexpensive solid-state processing route for synthesis of a wide range of novel materials such as nanocrystalline and amorphous alloys, nanostructured composites, and bulk metallic glasses.[1–5] Among other devices, MA is routinely carried out in planetary ball mills. The process involves high strain rate plastic deformation of a given powder charge within a confined volume that induces concomitant deformation, cold welding, fragmentation, interdiffusion, and dynamic recrystallization. In the recent past, the present group of authors have synthesized several Al-based amorphous and nanocrystalline alloys by MA.[6–9] The present report aims to demonstrate microstructural evolution in the course of the synthesis of Al + stainless steel powder composites by MA of either elemental powder blend with appropriate average composition or a mixture of aluminum and prealloyed stainless steel powder. This study is of interest for, apart from developing Al-based high specific strength composite, two separate practical applications: mechanical joining of aluminum with stainless steel (say, by friction welding or contact rolling) and prediction/simulation of microstructural damages/changes in stainless steel or aluminium-based coatings subjected to high strain rate wear or erosion. While joining metallic couples with restricted or no solubility and prone to formation of brittle intermetallic phases often necessitate joining of dissimilar metals/materials by mechanical force/pressure as an alternative to fusion welding, railroad or tribological coatings undergo degradation due to progressive friction and wear during prolong use. Microstructural and phase evolution in both the processes or degradations can be studied and simulated by subjecting the concerned material to high-energy ball milling.[10–12]

P.P. CHATTOPADHYAY, Professor, and A. SAMANTA, Scholar, are with the Department of Metallurgy and Materials Engineering, Bengal Engineering and Science University, Shibpur, Howrah 711 103, West Bengal, India. W. LOJKOWSKI, Professor, is with Unipress, Warsaw, Poland. H.-J. FECHT, Professor, is with the Division of Materials, University of Ulm, 89081, Ulm, Germany. I. MANNA, Professor, is with the Metallurgical and Materials Engineering Department, IIT, Kharagpur 721 302, India.

Manuscript submitted May 1, 2006.
Article published online August 9, 2007.

II. EXPERIMENTAL

Elemental powder (< 50-μm particle size) blends comprising appropriate amounts of Al, Fe, Cr, Ni, Mo, and C (> 99.5 wt pct purity), equivalent to AISI 316 stainless steel (316SS) composition, were subjected to MA by high-energy planetary ball milling in a Fritsch P6 planetary ball mill in wet (toluene) medium with a ball-to-powder ratio of 10:1 using WC vial and balls (10-mm diameter). Similar MA operation was carried out with powder mixtures comprising prealloyed 316SS (commercially available) and elemental aluminum powders in three different proportions (316SS + 25, 65, and 85 wt pct Al). For comparison, mechanical milling of prealloyed 316SS powder and elemental powder blend of Al, Fe, Cr, Ni, Mo, and C, equivalent to a mixture of 316SS (316ELSS) + 65 wt pct Al, was also carried out under identical condition. Milling in toluene prevented agglomeration of powders and welding of Al to the milling media (balls/vial). Following MA or milling, all the milled products were isothermally annealed at 775 K for 2 hours to relieve strain and study the probable microstructural change of the ball-milled samples at elevated temperature. The identity and sequence of phase evolution in different stages of MA as well as after isothermal treatment of the ball-milled products were

studied by the X-ray diffraction (XRD) technique using a PHILIPS* PW1830 diffractometer with Cu K_α (0.154-nm) radiation. The ball-milled samples (approximately 10 to 15 mg in each case) were subjected to differential scanning calorimetry (DSC) using a Mettler 4000 instrument under dynamic argon atmosphere at a heating rate of 4.88 K s^{-1} to examine their thermal stability. The average grain size (d_c) was determined from broadening of the most intense peak of the concerned phases using the Voigt method,[13] which allows judicious elimination of the contributions due to instrumental and strain effects in the observed peak broadening. It may be noted that Voigt analysis is based on the Scherrer principle of crystallite size determination using XRD analysis.[14] Selected powder samples were studied using a transmission electron microscope (TEM) in bright-field and high-resolution mode (high-resolution transmission electron microscopy (HRTEM)) using a PHILIPS CM-20 TEM instrument to verify the grain sizes and phase identity (using selected area diffraction (SAD)) obtained from XRD. The final ball-milled products of 316SS + Al (25, 65, and 85 wt pct) were subjected to isothermal compaction and sintering under 10 GPa pressure at 200 °C, 300 °C, and 400 °C. The scanning electron microscopy (SEM) of the consolidated sample was conducted using a JEOL** 5510 scanning electron microscope, and the hardness measurement was carried out with a Lietz miniload 2 Vickers tester at 981-mN load.

*PHILIPS is a trademark of Philips Electronic Instruments Corp., Mahwah, NJ.

**JEOL is a trademark of Japan Electron Optics Ltd., Tokyo.

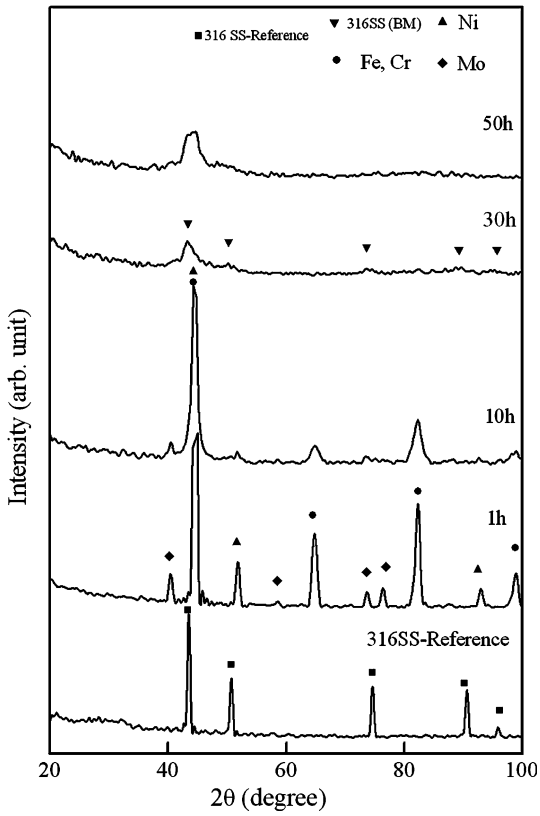

Fig. 1—XRD pattern obtained after ball milling of elemental blend having nominal composition comparable to 316SS. The XRD pattern of the 316SS alloy is appended as a reference for indexing the fcc ball-milled product after 30 h.

III. RESULTS

A. *Ball Milling*

Figure 1 shows the phase evolution in terms of XRD profiles obtained at appropriate stages of milling during MA of Fe + Cr + Ni + Mo + C elemental powder blend with 316SS-equivalent nominal composition. The XRD pattern obtained from commercial 316SS prealloyed powder is appended at the bottom as the reference for a direct comparison. The XRD pattern of the sample after 1 hour of MA comprises major peaks from α-Fe, Ni, Cr, and Mo. After 10 hours of ball milling, the peaks related to the α-iron become significantly broad, and the peak broadening analysis yields a grain size of 58 nm.[13,14] After 30 hours of ball milling, a new phase appears prominently in the XRD pattern having fcc Bravais lattice with concomitant disappearance of α-Fe. It may also be noted that the diffraction peaks concerning the new fcc phase appear at 2θ values, which are distinctly different than the 2θ values related to the diffraction peaks of fcc Ni. Moreover, the 2θ values related to the peaks in the XRD pattern of 30 hours of ball-milled sample reasonably matched with the corresponding peak positions in the XRD pattern of the reference 316SS alloy appended in Figure 1. The peak broadening analysis after appropriate corrections suggests that the fcc phase is nanocrystalline with an average grain size of 16 to 20 nm. Further analysis yields a lattice parameter of the fcc phase of 0.3577 nm, which compares well with that for 316SS. Therefore, it is evident that MA in the present ball-milling schedule has been successful in synthesizing nanocrystalline 316SS powder with fcc crystal structure and lattice parameter comparable to standard 316SS alloy rather than a Ni-rich solid solution. This also proves that MA has resulted into a structural transformation (bcc to fcc) of α-Fe by way of dissolution of Ni, Cr, Mo, and C in solid state to develop austenitic stainless steel from an elemental powder blend. This result is similar to that of Miura *et al.*[15] in respect to synthesizing high nitrogen Cr-Ni and Cr-Mn stainless steel powders by MA with partly alloyed powder blend. Figure 1 further reveals that continuation of ball milling of the austenite phase up to 50 hours increases peak width (indicating further grain refinement) but no further structural change (say, fcc to bcc or martensitic change).

Figure 2 shows microstructural changes in terms of the XRD patterns of prealloyed 316SS powders subjected to high-energy ball milling. The XRD pattern of the initial powder blend after 1 hour of milling is

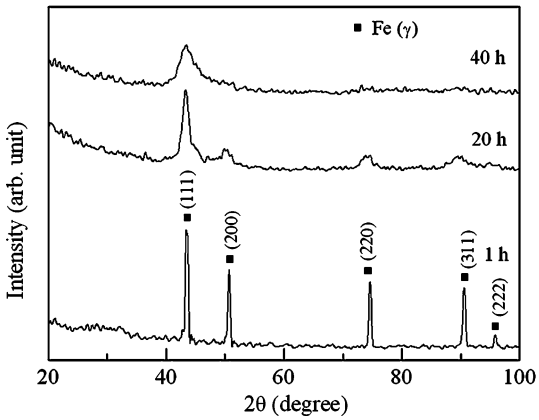

Fig. 2—XRD patterns of prealloyed 316SS powder blend subjected to ball milling for different cumulative milling times.

indexed as a single-phase fcc alloy with a lattice parameter value of 3.59 nm measured by extrapolating the Nelson–Riley parameter.[14] After 20 hours of ball milling, the peaks recorded a considerable amount of broadening, which corresponds to an average grain size value of 24 nm.[13,14] The XRD pattern of the sample obtained after 40 hours of milling shows the presence of a well-defined halo in the 2θ region related to the (111) reflection indicating a perceptible amount of amorphization of the powder blend after 40 hours of milling. However, the notable variations in the curvature at different 2θ values within the range of the halo is indicative of the presence of nanocrystalline phases in the partially amorphized powder blend. The peaks related to the higher order reflection completely disappear after 20 hours of milling. Further continuation of milling has not yielded any notable change in the XRD pattern of the powder blend indicating that perhaps complete amorphization or any further structural change of the 316SS powder is not possible under the present set of milling condition.

Figure 3 shows the XRD pattern of the powder blend comprising prealloyed 316SS and elemental Al (25 wt pct) after different ball milling durations. It is apparent that the intensity of the peaks concerned with Al is significantly reduced after 10 hours of ball milling. The peak broadening analysis indicates nanocrystallization of 316SS with an average grain size of 20 nm with concomitant dissolution of Al in 316SS. Continued MA of the blend has ensured complete dissolution of Al in 316SS ($d_c \cong 12$ nm) after 20 hours duration. Lattice parameter measurement of the fcc peaks indicated that dissolution of Al in the 316SS to a level of 25 wt pct does not result in any notable change. The large broadening in the first-order maxima in the XRD pattern of the 40 hours ball-milled product indicates partial amorphization of the alloyed phase. However, the presence of detectable intensity maximum concerned with the crystalline peaks in the XRD pattern is suggestive of incomplete amorphization at this stage. Further ball milling of the powder blend up to a duration of 50 hours significantly increased the width of the (111) peak region.

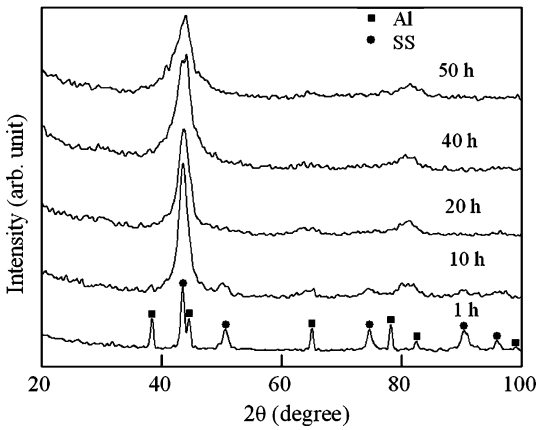

Fig. 3—XRD patterns of a powder mixture of 316SS and 25 wt pct Al subjected to planetary ball milling for different cumulative milling times.

Figure 4 shows the HRTEM image and SAD pattern of the ball-milled 316SS + 25 wt pct Al powder after MA for 50 hours and reveals the presence of a few crystalline regions (< 20 nm) within an amorphous matrix. The corresponding SAD pattern reveals rings arising out of the nanocrystalline regions along with the prominent halo due to the amorphous phase present in the matrix.

Figure 5 reveals the XRD pattern of the powder blends comprising 316SS + 65 wt pct Al after different ball milling durations. Peak broadening analysis of the pattern obtained after 10 hours of ball milling shows nanocrystallization of both elemental Al (60 nm) and 316SS (40 nm) without any significant alloying. Complete dissolution of Al in 316SS is obtained only after 30 hours of ball milling. An attempt to measure the grain size from the (111) peak yields an extremely small value (< 5 nm) of grain size and suggests the possibility

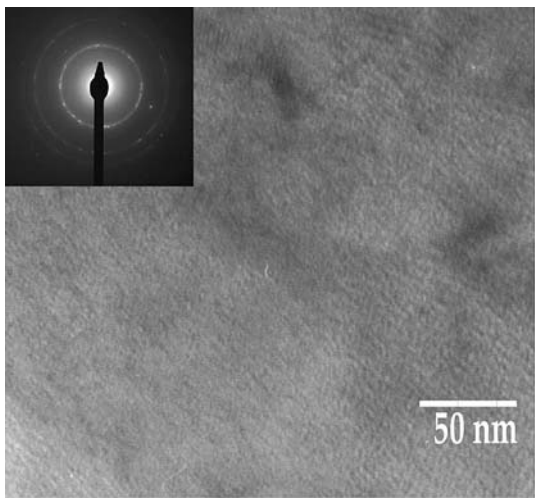

Fig. 4—HRTEM images of 316SS and 25 wt pct Al powder blend showing nanocrystalline grains following 50 hours of ball milling. The SAD (inset) pattern confirms the matrix as a nanocrystalline fcc phase.

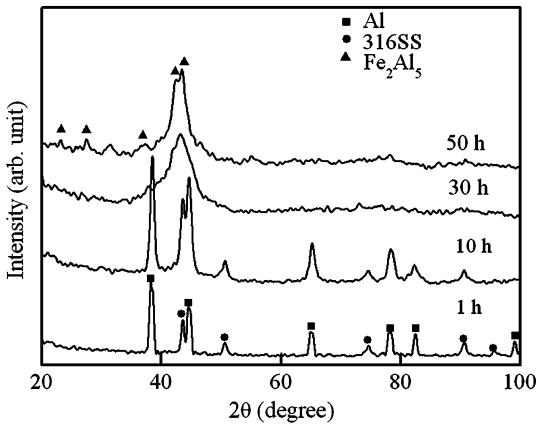

Fig. 5—XRD patterns of a powder mixture of 316SS and 65 wt pct Al subjected to planetary ball milling for different cumulative milling times.

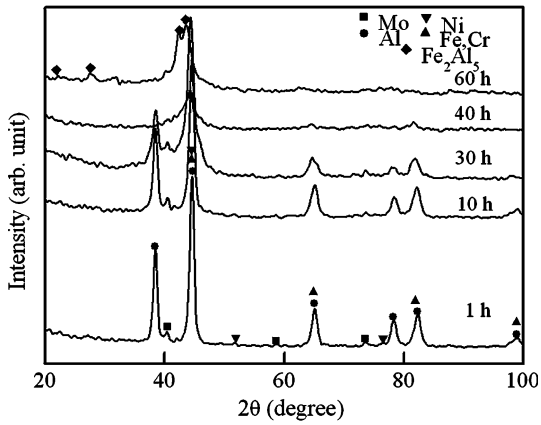

Fig. 7—XRD patterns of a powder mixture of elements with equivalent 316SS composition and 65 wt pct Al subjected to planetary ball milling for different cumulative milling time.

of amorphization of the ball-milled product at this stage. Subsequent ball milling up to a period of 50 hours results in a remarkable change in the XRD pattern due to primary crystallization of some nanocrystalline phase from the amorphous matrix, which may be indexed as $Fe_2 Al_5$.

Figure 6(a) reveals the HRTEM image of the 316SS + 65 wt pct Al mixture after ball milling of 30 hours and the corresponding SAD pattern (inset). It reveals the prominent presence of the amorphous phase with some presence of nanocrystalline region. The observation is corroborated by the clear appearance of the halo in the corresponding SAD pattern. However, a notable amount of nanocrystalline regions can be detected along with the amorphous phase in the HRTEM image, as shown in Figure 6(b). The corresponding SAD pattern exhibits the prominent appearance of the diffraction ring along with the halo, substantiating the fact that continuation of ball milling for a duration of 50 hours allows primary crystallization from the amorphous matrix.

Figure 7 shows the XRD patterns of the elemental powder blend of Fe + Cr + Ni + Mo + C (with 316SS equivalent composition) mixed with 65 wt pct Al after different duration of ball milling. It is apparent that almost all the elemental constituents are present in the blend even after ball milling for 30 hours in contrast to the results shown in Figure 1 where all the elements (Fe, Ni, Cr, Mo, and C) dissolved in the nanocrystalline fcc phase after 30 hours of MA. At this stage, the d_c of the Al phase attains a value of 28 nm, while the same for other constituents could not be measured due to overlapping of the concerned major peaks. Formation of a single-phase product was possible only after 40 hours of MA, resulting in an extremely broad first-order maxima in the XRD pattern similar to that obtained in the case of 316SS + 65 wt pct Al powder blend after 30 hours of ball milling (Figure 5). The formation of Fe_2Al_5 phase has only been achieved after MA of the present blend for a duration of 60 hours, in contrast to the results obtained in the case of MA of 316SS + 65 wt pct Al powder blend.

Figure 8 shows the HRTEM image of Fe + Cr + Ni + Mo + C (with 316SS equivalent composition) mixed with 65 wt pct Al after 60 hours of ball milling. The image reveals predominantly amorphous matrix with a notable amount of nanocrystalline regions, which

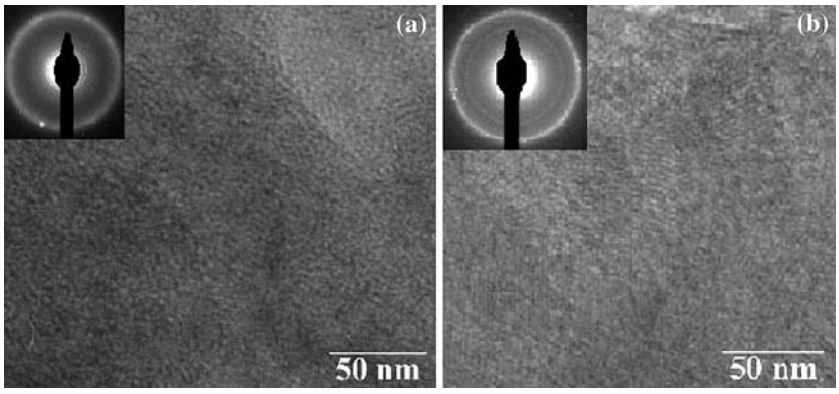

Fig. 6—(*a*) HRTEM images of 316SS and 65 wt pct Al powder blend showing predominantly amorphous microstructures following 30 h of ball milling and the corresponding SADP (inset). (*b*) HRTEM images of 316SS and 65 wt pct Al powder blend showing nanocrystalline grains following 50 h of ball milling. The SAD (inset) confirms the matrix as a nanocrystalline fcc phase.

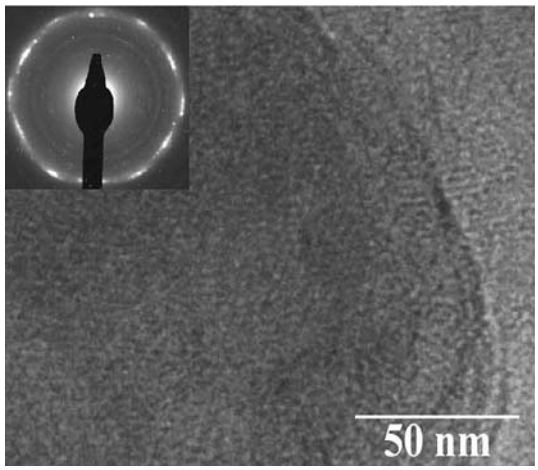

Fig. 8—HRTEM images of elemental SS316 and 65 wt pct Al powder blend showing predominantly amorphous structure following 60 h of ball milling. The SAD (inset) pattern confirms the matrix as a nanocrystalline fcc phase.

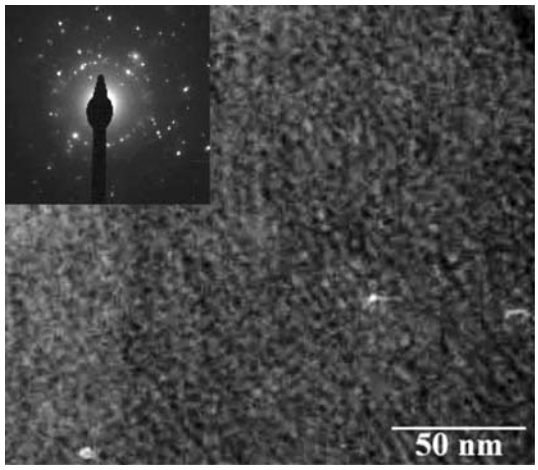

Fig. 10—HRTEM images of elemental 316SS and 85 wt pct Al powder blend showing predominantly nanocrystalline structure following 50 h of ball milling. The SAD (inset) pattern confirms the matrix as a nanocrystalline fcc phase.

is further evident from the SAD pattern showing the prominent presence of the diffraction ring along with the halo.

Thus, comparison of the results shown in Figures 5 through 8 demonstrates that ball milling 316SS and 316ELSS powder blends, respectively, containing 65 wt pct Al result in a similar sequence of phase evolution, with slightly delayed kinetics in the case of the latter.

Figure 9 reveals the XRD patterns of the powder blend of 316SS alloy containing 85 wt pct Al after different ball milling durations. Nanocrystallization of the Al (d_c = 68 nm) and 316SS (d_c = 44 nm) phases was achieved after ball milling for 15 hours. Continuation of ball milling for a period of 30 hours results in further reduction in grain size of Al (d_c = 28 nm) and 316SS (d_c = 19 nm). The XRD pattern of the sample obtained after 50 hours of ball milling seems closely comparable to that obtained after 30 hours without the extent of peak broadening usually associated with amorphization. Thus, Figure 9 demonstrates that ball milling of the powder blend of 316SS alloy containing 85 wt pct Al results into a composite microstructure comprising nanocrystalline Al phase dispersed in the nanocrystalline 316SS alloy matrix after attaining the steady state of phase evolution.

Figure 10 shows the HRTEM image of 316SS mixed with 85 wt pct Al after 50 hours of ball milling. The micrograph reveals a predominantly crystalline matrix. This is further evident from the SAD pattern showing the prominent presence of diffraction spots along with the diffraction ring, indicating that the matrix comprises nanocrystalline as well as coarse crystalline phases.

B. *DSC Analysis*

Figure 11 shows the DSC thermograms obtained from ball-milled 316SS + 65 wt pct Al powder blend. The exothermic peaks appearing below 600 K are detected in the case of the entire ball-milled samples subjected to the DSC experiment. In analogy to the

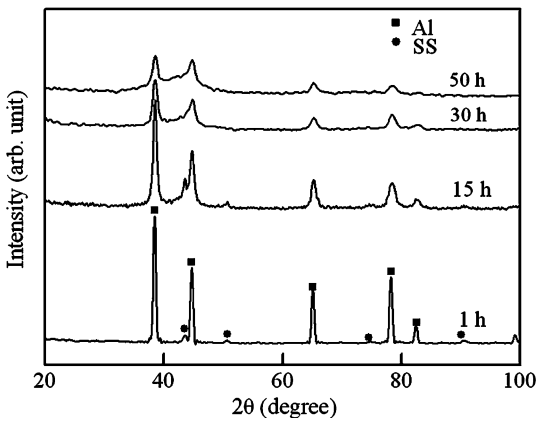

Fig. 9—XRD patterns of a powder mixture of 316SS and 85 wt pct Al subjected to planetary ball milling for different cumulative milling times.

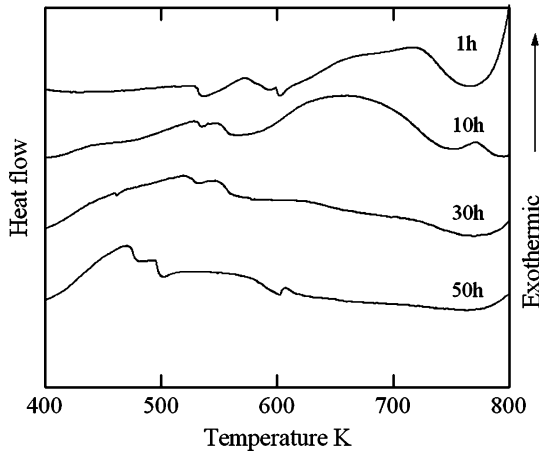

Fig. 11—DSC patterns of 316SS with 65 wt pct Al alloy powder during ball milling for different intervals.

earlier results,[16] the concerned peaks may be attributed to the thermally activated microstructural activities involving various kinds of defect structures. The broad exothermic region in the thermogram of samples ball milled for 1 and 10 hours appearing between 600 and 800 K is due to nucleation of the crystalline Fe_2Al_5 phase. It is interesting to note that the DSC thermogram concerning samples collected after 30 and 50 hours of ball milling does not exhibit the appearance of the broad exothermic peak between 600 and 800 K, due to formation of Fe_2Al_5 phase earlier in the powder blend after 30 hours of ball milling. Therefore, the ball-milled powders sampled for 30 hours and beyond do not exhibit any prominent response to the thermally activated changes during the DSC experiment with respect to phase transformation.

Figure 12 compares the phase evolution among 25, 65, and 85 wt pct Al containing 316SS powder blends after ball milling for 50 hours. It is evident that in the 25 wt pct Al containing sample, some exothermic peaks appear between 550 and 800 K, which can be attributed to the formation of the Fe_2Al_5 phase. In the case of the 85 wt pct Al containing sample, the sharp peaks of smaller intensities formed at the lower temperature regime are possibly due to thermally activated microstructural activities taking place in Al-rich and Fe-rich phases and thus appearing at different temperatures. On the other hand, the broad peak with higher intensity is formed due to overlapping intensities of exothermic peaks due to crystallization of the Al-rich phase and intermetallic phase.

C. *Isothermal Treatment of Ball-Milled Sample*

Figure 13 presents the XRD pattern of ball-milled 316SS powder blends containing 25, 65, and 85 wt pct Al after subjecting them to isothermal treatment at 775 K for 2 hours. All of the XRD pattern demonstrates almost complete crystallization of the ball-milled powder blends. The XRD pattern obtained from 25 wt pct Al containing 316SS powder blend allowed indexing of one set of peaks as Fe_3Al, while the remaining

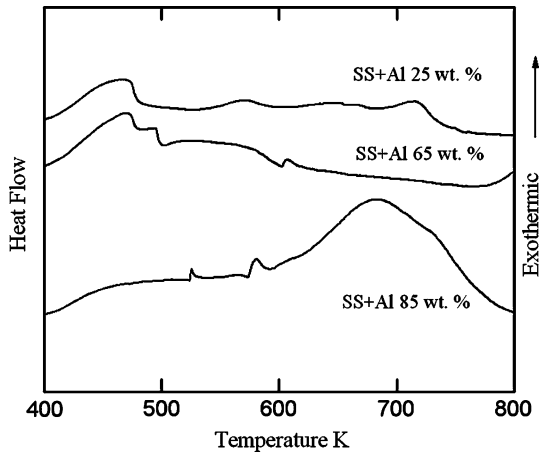

Fig. 12—DSC patterns of 316SS with 25, 65, and 85 wt pct Al alloy powder after ball milling of 50 h.

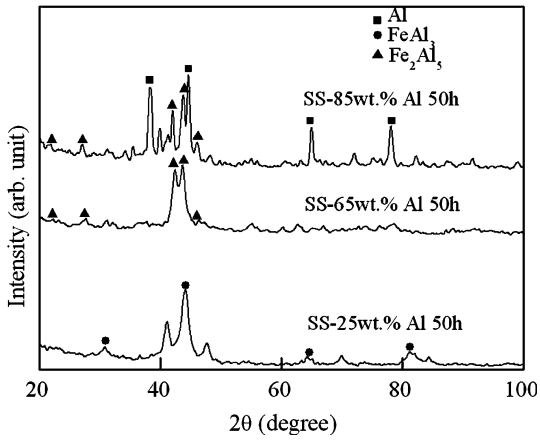

Fig. 13—XRD patterns of the ball-milled samples after isothermal treatment at 775 K for 2 h.

crystalline peaks could not be matched with the phase expected to form in case of the concerned alloys. Ball-milled samples of the 65 wt pct Al containing 316SS sample clearly demonstrate the formation of ordered Fe_2Al_5 phase. Isothermal annealing of the sample containing 85 wt pct Al resulted in crystallization of Fe_2Al_5 and an Al-rich solid solution. Therefore, it is evident that the current alloys undergo complete crystallization under the selected thermal treatment schedule.

D. *Consolidation of the Ball-Milled Products*

Figures 14(a) through (c) show the XRD pattern obtained from the ball-milled and compacted (at different temperatures) products of powder blends of 316SS alloy containing 25, 65, and 85 wt pct Al, respectively. Figure 14(a) shows that the compacted 316SS + 25 wt pct Al sample comprises a mixture of nanocrystalline and amorphous phases over the range of consolidation temperature. Similarly, Figure 14(b) suggests that the compacted 316SS + 65 wt pct Al sample comprises Fe_2Al_5 phase with a slight tendency of grain coarsening at 400 °C. In the case of the 316SS + 85 wt pct sample (Figure 14(c)), it appears that the consolidated samples maintain a composite microstructure of nanocrystalline Al and the fcc phase over the entire temperature range of consolidation.

Figures 15(a) through (c) show the SEM micrographs of green compacted alloys containing 85, 65, and 25 wt pct Al, respectively. It is apparent that the sample containing 85 wt pct Al forms large porous chunks with small porous particles adherent to it. The average size of the chunks with fairly dense appearance is reduced in the sample containing 65 wt pct Al. In the case of compacted samples containing 25 wt pct Al, the amount of porosity within the chunks is remarkably reduced with a fairly smooth and dense appearance of the surface.

Figures 16(a) through (c) present the SEM micrograph obtained from the as-polished surface of the hot-compacted alloys containing 25 wt pct, 65 wt pct, and 85

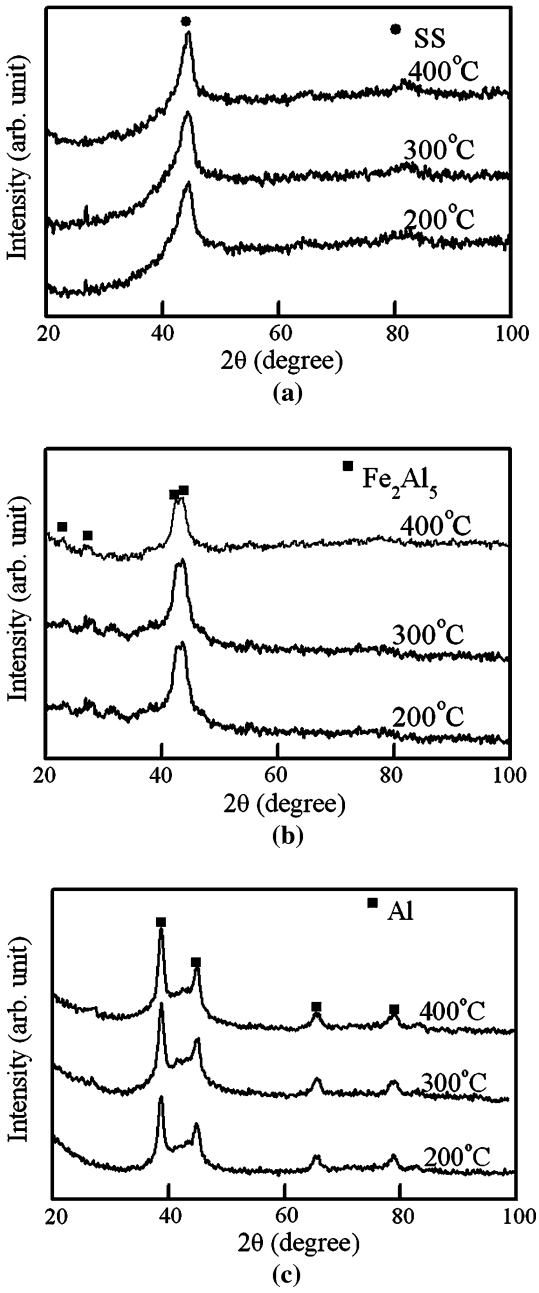

Fig. 14—XRD patterns of compacted samples at different temperatures: (*a*) 316SS + 25 wt pct Al, (*b*) 316SS + 65 wt pct Al, and (*c*) 316SS + 85 wt pct Al.

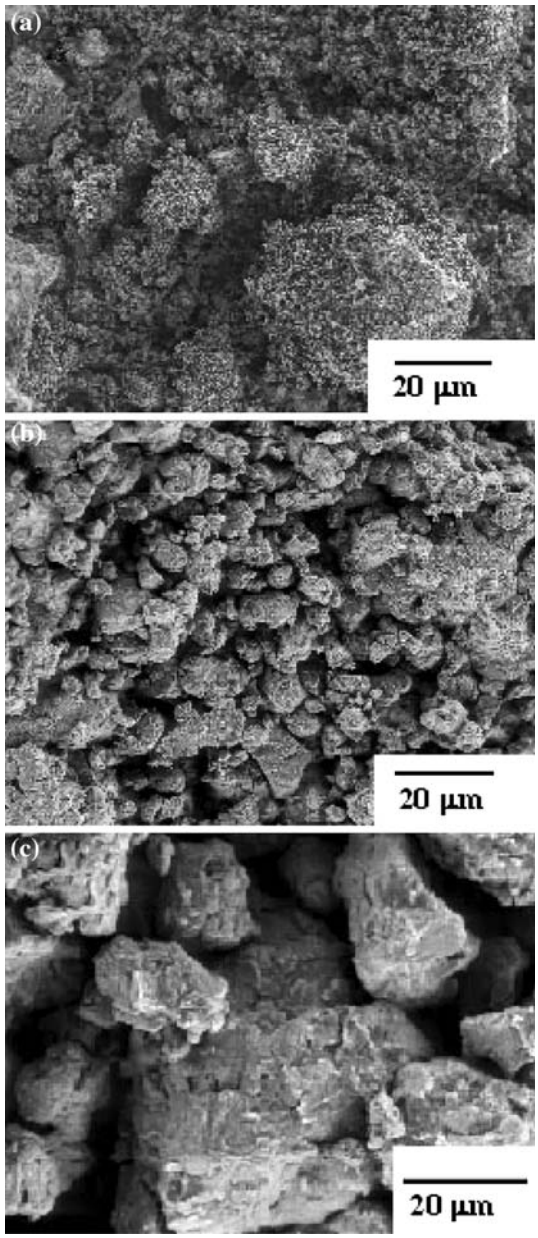

Fig. 15—Scanning electron micrograph of green-compacted samples of powder blends consisting of (*a*) 316SS + 85 wt pct Al, (*b*) 316SS + 65 wt pct Al, and (*c*) 316SS + 25 wt pct Al.

wt pct Al, respectively. Figure 16(c) reveals evidence of deformation of the ductile particles along with the presence of porosities within the particles and discontinuities along the interfaces between the particles. The SEM observation of the green-compacted and hot-consolidated samples indicates that a higher volume fraction of the ductile constituent results in an inhomogeneous flow pattern, leading to a consolidated mass containing porosities and discontinuities. On the other hand, the flow pattern in the single-phase powder blends achieved in samples containing 65 wt pct and 25 wt pct Al, due to deformation under compressive pressure, is fairly homogeneous, leading to the formation of consolidated mass practically devoid of porosity and discontinuities.

Figure 17 presents the hardness values obtained from samples containing 316SS alloy containing 25, 65, and 85 wt pct Al, respectively, after consolidation at different temperatures. It is apparent that the hardness values obtained after consolidation at different temperatures increase in the order of 316SS alloy containing 85 wt pct Al, 25 wt pct Al, and 65 wt pct Al. For 316SS alloy containing 25 wt pct Al and 316SS alloy containing 65 wt pct Al, the hardness values decrease marginally while a notable decrease in the same is recorded for 316SS

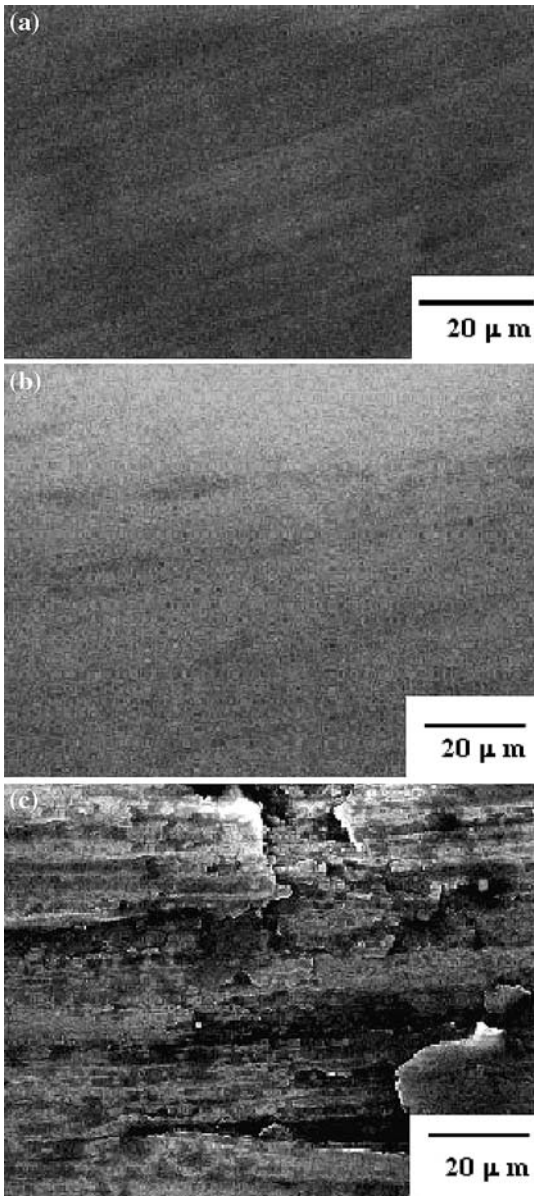

Fig. 16—SEM micrographs of hot-compacted samples of 316SS alloy with (*a*) 25 wt pct Al, (*b*) 65 wt pct Al, and (*c*) 85 wt pct Al.

alloy containing 85 wt pct Al when the consolidation temperature increases from 300 °C to 400 °C.

IV. DISCUSSION

A. *Ball Milling*

Results of MA/ball milling of 316SS alloy powders have resulted in extreme disordering, leading to nanocrystallization/amorphization of the ball-milled product. In the case of 316ELSS powder blend, the bcc iron has been subjected to deformation-induced alloying followed by a bcc to fcc transformation, which resulted in similar ball-milled product, as in the case of 316SS. In the absence of adequate thermal energy during ball milling, alloying may be considered to be driven by

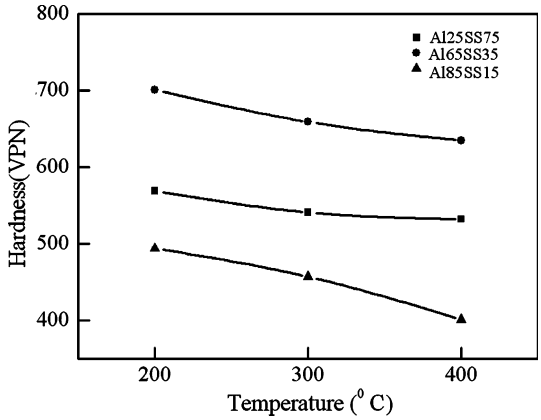

Fig. 17—Hardness values of different alloy systems after compaction at different temperature.

dissipation of excess energy acquired due to creation of a high volume fraction of interfacial area and an increased amount of configurational entropy in the system.[17] Albeit the absence of solubility data between Al and fcc Fe during ball milling, formation of the amorphous phase in the Al-Fe system over a wide composition range has earlier been predicted in several ball milling experiments and theoretical prediction using Mediema's semiempirical model.[18,19] It is evident from Figures 3 through 10 that Al preferentially dissolves into fcc Fe, leading to the formation of nanocrystalline or amorphous phase. It is reasonable to envisage that at the initial stage of ball milling, Al is deformed preferentially spreading over the relatively harder particles of 316SS. The 316SS particles deform only after sufficient deformation of Al, allowing the defect-induced dissolution of Al into the fcc particles. The results of EDS analysis of different ball-milled products, as presented in Table I, indicate that the ratio of the constituent elements in the final ball-milled product is close to the ratio of elements in the initial powder blend. Such an observation indicates uniform mixing of the constituent elements in spite of the difference in respect of their densities. Such a feature inherent in the process of ball milling resulted in a ball-milled product with a reasonable extent of homogeneity. It may be noted here that in the present ball milling experiments, formation of an intermediate phase such as Fe_2Al_5 is favored over others such as $FeAl_3$, in spite of the favorable stoichiometry in some of the blends. It may be mentioned here that preferential formation of Fe_2Al_5 during ball milling of the Al-Fe powder blend under similar milling conditions has been previously demonstrated.[19] Earlier ball milling experiments in various alloy systems have also demonstrated that, while some intermetallic phases form during ball milling and remain stable after prolonged milling, others do not form easily. However, possibilities in respect of the formation or stability of a particular intermetallic phase *vis-á-vis* amorphous/solid solution phase during ball milling of a given composition are inconspicuous to date. In this regard, it may be conjectured that the subcritical nucleus of the high density intermetallic phase, which forms within the

Table I. EDS Analysis Result of Final Ball-Milled Product of Different Powder Blends

Blends	Elements (Wt Pct)				
	Al	Fe	Cr	Ni	Others*
Elemental SS	—	72.00	19.00	9.00	nil
316-SS + 25 wt pct Al	18.94	51.64	10.48	7.88	11.06
316-SS + 65 wt pct Al	54.69	20.71	4.25	3.44	16.91
316-SS + 85 wt pct Al	70.35	10.00	2.33	1.80	15.52

*Includes impurity/light elements such as W, C, Mn, Si, Mo, *etc.*

disordered solid solution or amorphous matrix, results in a difference in density across the interface between the matrix and the subcritical particle. As proposed earlier, the difference in density may be interpreted in terms of the difference in volume of mixing per atom in the intermetallic phase and the solid solution of identical composition (ΔV_{mix}).[20] This difference may result in difficulties in attaining the coherency at the interface, which is essential to compensate the high amount of interfacial energy associated with the nucleation of very fine crystalline phase within a matrix of reduced volume.[17] While lower volume per atom of the dense intermetallic in comparison with the solid solution (obtained by Vegard's law) indicates greater difficulties for the formation of the intermetallic phase within the amorphous matrix, comparable values of volumes per atom of the intermetallic phase and the solid solution favor the formation of intermetallic phase. Figure 18 shows that, among the intermediate phases present in the Al-Fe phase diagram, Fe_2Al_5 has the lowest value of ΔV_{mix}, or, in other words, Fe_2Al_5 has comparable volume per atom with that of the solid solution of identical composition. This indicates that primary crystallization of Fe_2Al_5 from a solid solution/amorphous matrix is favored among the intermetallic phases in the Fe-Al system during ball milling. Therefore, it is suggested that the difference in atomic volume between the solid solution and the intermetallic phase corresponding to a given composition may be considered as one of the important factors in respect to the possibility of primary crystallization of the Fe_2Al_5 phase from a disordered solid solution or an amorphous phase.

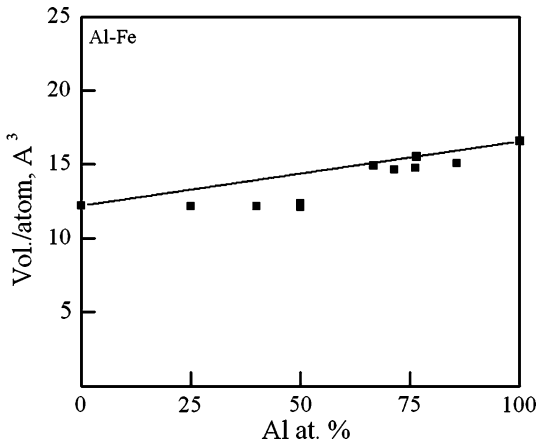

Fig. 18—Deviation of atomic volume from Vegards' law of the compounds of the relevant Al-Fe binary system.

B. *Consolidation of the Ball-Milled Products*

It is interesting to note that the present hot consolidation technique has not allowed any notable coarsening or phase change of the constituent phases present in the ball-milled powder blend (Figure 14). However, the degree of peak broadening is somewhat reduced with the increase in consolidation temperature from 200 °C to 400 °C without any significant variation in the nature of the constituent phases.

The comparison of the SEM micrographs of the green-compacted and hot-consolidated samples indicates that better consolidation has been achieved in the case of single-phase powder blend rather than that comprising a composite mixture of ductile Al and hard SS solid solutions possibly due to the difference in straining behavior of the constituent phases in the case of the letter. On the other hand, comparison between hardness values (Figure 17) and the microstructure (Figure 16) confirms that the hot-compacted samples are nearly pore free and considerably dense. The hot-consolidated samples with a composite microstructure of amorphous and nanocrystalline phases seem to possess higher hardness values than those containing nanocrystalline intermetallic phase or a mixture of nanocrystalline solid solutions.

V. CONCLUSIONS

1. Ball milling of 316SS powder blends resulted in a composite microstructure comprising amorphous and nanocrystalline phases. Complete amorphization has not been achieved even after prolonged ball milling.
2. Ball milling of elemental powder blend of composition equivalent to that of 316SS demonstrated the transformation of bcc iron to fcc solid solution comparable to 316SS by dissolution of alloying elements.
3. Aluminum has dissolved completely in fcc lattice of 316SS up to 65 wt pct. A significant amount of Al remained undissolved in the case of powder blend comprising 316SS and 85 wt pct Al. Dissolution of 65 wt pct Al resulted into complete amorphization

of the solid solution after 30 hours of ball milling. Continuation of ball milling of 316SS + 65 wt pct Al resulted in crystallization of Fe_2Al_5 phase.

4. Atomic level mixing during ball milling has been ensured by the fact that elemental blends comprising the constituents of 316SS have undergone homogeneous mixing to the extent that resulted in formation of fcc phase equivalent to 316SS. This is further evidenced by the EDS results of the ball-milled products.
5. Powder blend comprising Al and constituent elements of 316SS resulted in formation of nanocrystalline bcc solution with the lattice parameter comparable with elemental Fe.
6. Cold compaction followed by high-pressure sintering produces bulk metastable Al-316 SS alloy with almost 100 pct density. The bulk-consolidated materials have exhibited formation of homogeneous microstructure. The ball-milled powder blend with single-phase microstructure yielded better consolidation behavior as compared with the multiphase powder blends.
7. A superior hardness value has been achieved in the case of the consolidated sample comprised of 316SS and 65 wt pct Al. The average hardness value is significantly greater than either Al or 316SS.

ACKNOWLEDGMENTS

Financial support from the Council of Scientific and Industrial Research (CSIR, Delhi, Sanction No. 22(336)/02/EMR-II) is gratefully acknowledged. Useful technical discussion with Dr. F. Banhart is greatly appreciated.

REFERENCES

1. H.J. Fecht: in *Nanostructured Materials–Processing, Properties, and Applications*, C.C. Koch, ed., Noyes Publication, William Andrew Publishing, Norwich, NY, 2002, pp. 73–114.
2. C. Suryanarayan: *Progr. Mater. Sci.*, 2001, vol. 46, pp. 1–184.
3. I. Manna, P. Nandi, B. Bandyopadhyay, K. Ghoshray, and A. Ghoshray: *Acta Mater*, 2004, vol. 52, pp. 4133–42.
4. C.C. Koch, O.B. Cavin, C.G. McKamey, and J.O. Scarbrough: *Appl. Phys. Lett.*, 1983, vol. 43, pp. 1017–19.
5. M. Sherif El-Eskandarany, Satoru Ishihara, Wei Zhang, and A. Inoue: *Metall. Mater. Trans. A,*, 2005, vol. 36A, pp. 141 –48.
6. I. Manna, P. Nandi, and P.M.G. Nambissan: *Phil. Mag. A*, 2004, vol. 84, pp. 3585–98.
7. I. Manna, P.P. Chattopadhyay, F. Banhart, and H.-J. Fecht: *Mater. Sci. Eng. A*, 2004, vol. A379, pp. 360–67.
8. I. Manna, P.P. Chattopadhyay, F. Banhart, and H.-J. Fecht: *Mater. Lett.*, 2004, vol. 58, pp. 403–07.
9. I. Manna, P.P. Chattopadhyay, F. Banhart, and H.-J. Fecht: *Z. Metallkd.*, 2003, vol. 94, pp. 835–41.
10. I. Manna, P.P. Chattopadhyay, F. Banhart, J. Croopnick, and H.-J. Fecht: *Wear*, in press.
11. W. Lojkowski, M. Djahanabakhsh, G. Buerkle, S. Gierlotka, W. Zielinski, and H.-J. Fecht: *Mater. Sci. Eng. A*, 2001, vol. 303, pp. 197–98.
12. D.A. Rigney, L.H. Chen, M.G.S. Naylor, and A.R. Rosenfield: *Wear*, 1984, vol. 100, pp. 195–219.
13. T.H. Keijser, I.L. Langford, E.J. Mittemeijer, and B.P. Vogel: *J. Appl. Cryst.*, 1982, vol. 15, pp. 308–14.
14. B.D. Cullity: *Elements of X-ray Diffraction*, Addison-Wesley, New York, NY, 1975, pp. 101–05.
15. H. Miura, H. Ogawa, and K. Omuro: *Mater. Sci. Forum*, 1999, vols. 318–320, pp. 707–14.
16. H. Bakker, G.F. Zhou, and H. Yang: *Progr. Mater. Sci.*,, 1995, vol. 39, pp. 159–241.
17. A.Y. Badmos and H.K.D.H. Bhadeshia: *Mater. Trans.*, 1997, vol. 28A, pp. 2189–94.
18. A.K. Niessen, F.R. de Boer, R. Boom, P.F. de Chatel, W.C.M. Mattens, and A.R. Miedemma: *CALPHAD*, 1983, vol. 7, pp. 51–70.
19. D.K. Mukhopadhyay, C. Suryanarayana, and F.H. Froes: *Scripta Metall. Mater.*, 1994, vol. 31, pp. 333–38.
20. A.R. Yaveri and A. Inoue: *Mater. Res. Soc. Symp. Proc.*, 1999, vol. 554, pp. 21–30.